Materials Research Proceedings 44 (2024) 320-329 https://doi.org/10.21741/9781644903254-34

Deformation laws and design method of near-net rolling for L-section rings with profile axial conical rolls

QIAN Dongsheng[1,2,3,a], GU Yixuan[1,2,b] , DENG Jiadong[2,3,c,*] and WANG Feng[1,2,3,d]

[1]School of Materials, Wuhan University of Technology, Luo Shi Road 122, 430070 Wuhan, China

[2]Hubei Key Laboratory of Advanced Technology for Automotive Components al. Luo Shi Road 122, 430070 Wuhan, China

[3]Hubei Engineering Research Center for Green Precision Material Forming al. Luo Shi Road 122, 430070 Wuhan, China

[a]qiands@whut.edu.cn, [b]gyx849757@163.com, [c]dengjd@whut.edu.cn, [d]wangfengwhut@163.com

Keywords: L-Section Rings, Near-Net Ring Rolling, Near-Net Rolling, FE Simulation, Ring Rolling Experiment

Abstract. L-section rings are widely used in key basic parts, such as flanges and rotary supports. When the radial length of the ring step is large while the axial depth is shallow, traditional ring rolling with profile mandrel may result in forming defects such as incomplete filling of the steps. This paper proposes a near-net rolling technology for L-section rings with profile axial conical rolls. Firstly, a finite element model for the rolling process of L-section ring was established. Then the revolution laws of the ring geometric dimension and the metal flowing behavior during the rolling process with profile axial conical rolls were studied. Further, the influence of key process parameters on the forming effects was revealed, including radial-to-axial deformation ratio, rolling ratio, and roller motion. Finally, the feasibility of the proposed process method was verified by FE simulation and rolling experiments. The research results provide a technical guidance for the near-net rolling forming of L-section ring, contributing to the high-performance, efficient, and cost-effective manufacturing of parts like L-section flanges and rotary supports.

Introduction

Ring rolling is an international mainstream technology for manufacturing high-performance large seamless rings, widely used in aviation, aerospace, automotive, engineering machinery, wind power, nuclear power and other fields, such as aviation casing rings, rocket storage tank rings, wind power bearing rings, etc. These ring components usually have complex structural shapes. However, in order to simplify the manufacturing process, rectangular or simple shaped section ring forgings are usually rolled, and then the target section shape is obtained through a large amount of cutting processing. This process not only has low material utilization and long processing cycles, but also weakens the mechanical properties of the product. Near-net rolling is an urgent need to achieve high-performance, high-efficiency, and low-cost manufacturing of such complex annular components, and it is also the forefront of research in the manufacturing technology of complex annular components for major equipment in aviation, aerospace, and wind power.

Compared to the rolling of rectangular section rings, the rolling process of irregular section rings is more complex, and there is relatively less research on it. D. S. Qian [1] designed four different ring blanks and determined the optimal blank design for the stepped section ring through theoretical analysis, finite element simulation, and experiments. Yu-Min Zhao [2] discussed the

impact of rolling ratio on the forming outcomes of groove section rings and identified a suitable rolling ratio range.Lin Hua [3] first used constraining ring rolling technique to form a conical ring with thin walls and three high ribs, and studied the metal flow behavior during the constrained ring rolling process.Lei Lian [4] proposed and applied an advanced feeding strategy driven by staged growth velocity, which improved the rolling stability and forming quality of groove section ring rolling.

As a typical irregular section ring, the L-section ring has important applications in key components for wind turbine flanges and bearings. It consists of a large rectangular ring and a small rectangular ring, that combine to form an L-section ring[5]. When using shaped mandrel to directly roll and form L-shaped rings, as shown in Fig. 1, if the step length is large while the axial depth is shallow, forming defects such as incomplete filling and folding at the step are prone to occur [6].

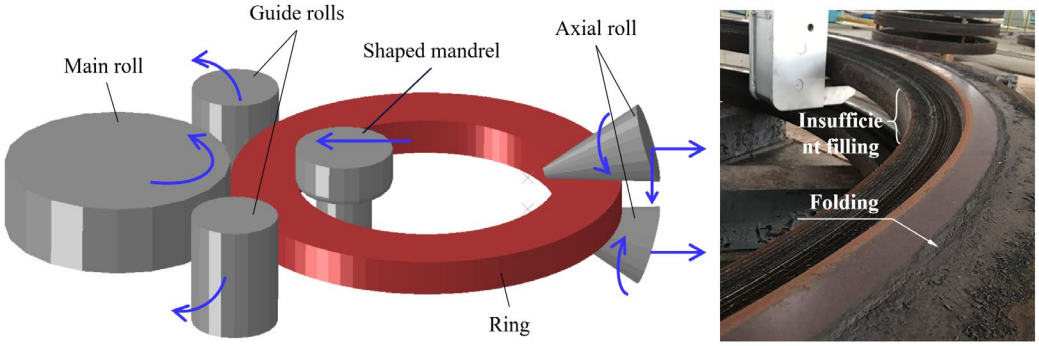

Fig. 1. L-section ring rolling with shaped mandrel.

For L-shaped section rings with large step lengths and shallow axial depths, profile axial conical roll can be used for near-net rolling, as shown in Fig. 2. This process utilizes an shaped axial roll with steps and utilizes the axial rolling pass to achieve direct rolling forming of L-rings [7]. During the rolling process, while the upper and lower cone rollers form the upper and lower surfaces of the ring axially, it is also necessary to ensure that the backward speed matches the growth speed of the outer diameter of the ring. By adding a pair of guide rolls on both sides of the axial rolls, the stability control of the ring rolling process is increased [8,9].

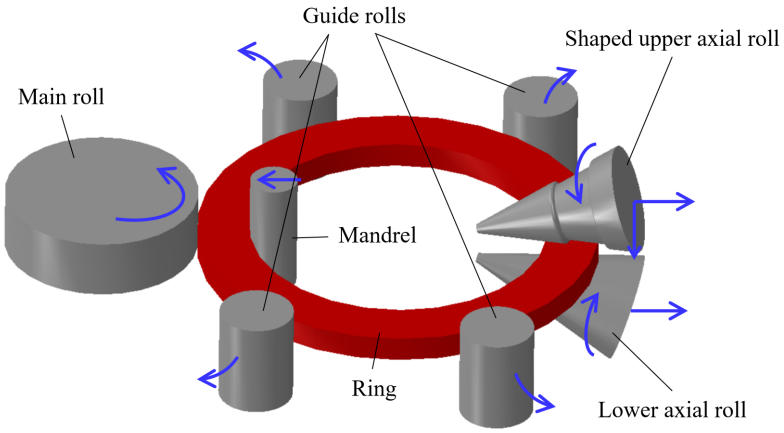

Fig. 2. Near-net shape rolling principle of L-section ring with profile axial conical rolls.

This article takes the L-section forging of a wind power yaw bearing as the research object. By establishing a finite element model for the rolling of L-section rings, the deformation law of the rings during the rolling process with profile axial conical rolls is analyzed, and the influence of key process parameters on the rolling forming is revealed, providing technical guidance for the near-net rolling of L-section rings.

Design of ring rolling process and FE modeling

Blank size design. The geometric relationship between the ring blanks and the forgings in the near-net rolling of L-section rings is shown in Fig. 3. Among them, H0 and B0 are the blank wall thickness and axial height of the ring, Bb and Bs are the axial height of the large hole section and the small hole section of the ring, Hb and Hs are the wall thickness of the large hole and the small hole of the ring, wherein the wall thickness and height of the large hole section of the ring are the key dimensions for the forming of the L-section ring. The shaped upper axial roll is pressed down to obtain the large hole part height Bb. And in order to ensure that the wall thickness of the large hole part of the L-section ring meets the design requirements, the shaped part of the upper axial roll should be kept away from the outer diameter of the ring Hb during the rolling process, so the backward speed of the cone roll VW and the growing speed of the outer diameter of the ring VD should meet the following definitions:

$$V_D = dD/dt. \tag{1}$$

$$V_W = V_D. \tag{2}$$

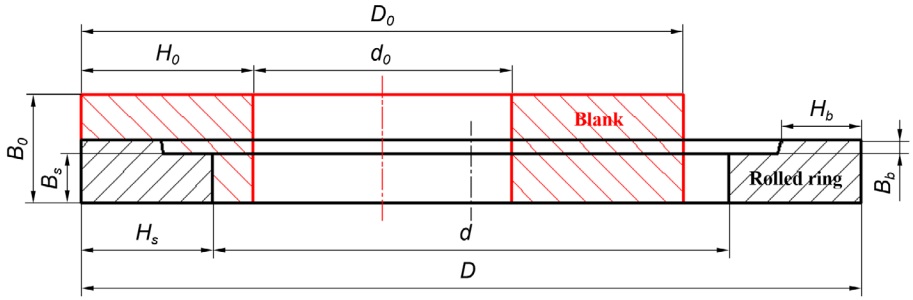

Fig. 3. Geometric relationship between ring blanks and forgings.

The specific parameters of L-section forging of wind power yaw bearing are shown in Table 1.

Table 1. Forgings dimension parameters（mm）.

D_s	B_b	B_s	H_s	H_b
3711	30	114	306	186

In the rolling process of irregular section ring, the main factor affecting the filling of section profile is the shape and size of the blank. Reasonable design of the blank size is the key to ensure the metal flowing and filling of L-section forgings [10,11].

The rolling ratio is an important parameter in the blank size design, which determines the deformation degree of the ring. For non-rectangular section ring rolling, the selection of rolling ratio has a greater impact on the filling of the section profile, and the L-section ring rolling ratio λ is defined as follows:

$$\lambda = \frac{A_0}{A} = \frac{H_0 B_0}{H_b B_b + H_s B_s}. \tag{3}$$

In radial-axial ring rolling (RARR) of L-section ring, the reduction ratio of blank wall thickness and height of ring parts, that is, radial-to-axial deformation ratio η, has an important influence on the forming degree of step inside ring parts. η is determined by the formula:

$$\eta = \frac{\Delta h}{\Delta b} = \frac{H_0 - H_s}{B_0 - B_s} = \frac{B_b + B_s}{H_s}. \quad (4)$$

Where Δh=H0-Hs、Δb=B0-Bs are radial and axial feeds respectively.

In order to study the influence of ring blank size on the shaped axial roll near-net rolling, two groups of 9 ring blank were designed for finite element numerical simulation experiments. The size parameters of ring blank are shown in Table 2. Group 1: In order to study the effect of the ratio of radial and axial feeds on the near-net rolling with shaped axial roll, η values of ring blank 1, 2, 3, 4 and 5 were selected as 0.28, 0.47, 0.69, 0.96 and 1.31, respectively, and the outer diameters of ring parts were 2700mm, and the rolling ratio was basically unchanged. Group 2: In order to study the effect of rolling ratio on the near-net rolling with shaped axial roll, the radial feed Δh of ring blank 6, 7, 3, 8 and 9 were selected as 61 mm, 51 mm, 42 mm, 34 mm and 26 mm, the axial feed Δb were 61 mm, and the rolling ratio λ were 1.58, 1.54, 1.50, 1.47 and 1.43, respectively.

Table 2. Dimensions of ring blanks.

Blank number	D_0/mm	H_0/mm	B_0/mm	η	Mandrel feed speed Vc/mm s^{-1}	Upper axial roll feed speed Va/mm s^{-1}	Rolling time /s	λ
1	2700	326	185	0.28	0.17	0.59	120	1.49
2	2700	337	180	0.47	0.26	0.55	120	1.50
3	2700	348	175	0.69	0.35	0.51	120	1.50
4	2700	360	170	0.96	0.45	0.47	120	1.51
5	2700	373	165	1.31	0.56	0.43	120	1.52
6	2600	367	175	1.00	0.51	0.51	120	1.58
7	2650	357	175	0.84	0.43	0.51	120	1.54
8	2750	340	175	0.56	0.28	0.51	120	1.47
9	2800	332	175	0.43	0.22	0.51	120	1.43

FE modeling. Based on the working principle of RARR, the 3D coupled thermo-mechanical FE model of L-section ring rolling with shaped axial roll was established by ABAQUS/Explicit program, as shown in Fig. 4. In the FE model, the ring part is set as a deformable body, the rolls are set as a rigid body, and the ring material is 42CrMo. The material constitutive equation and thermodynamic physical property parameters of the material are referred to paper[10]. The grid type is C3D8RT and dynamic explicit finite element algorithm is used to improve the computational efficiency. At the same time, ALE adaptive meshing is used to control mesh distortion in the deformation process. Other rolling parameters are shown in Table 3.

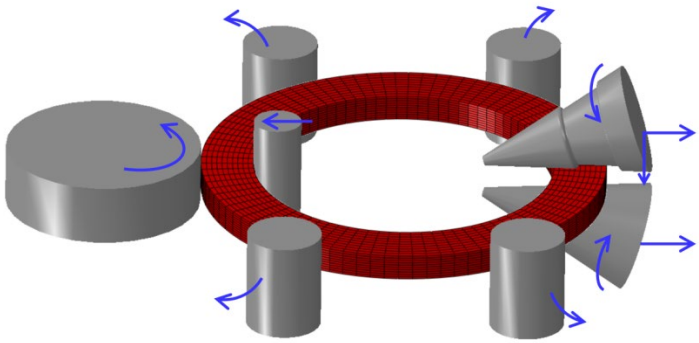

Fig. 4. FE model of L-section ring rolling with profile axial conical rolls.

Table 3. Simulated rolling parameters table.

Rolling parameter	value
Ring material	**42CrMo**
Driving roll working radius	**650mm**
Core roll working radius	**160mm**
Guide roll radius	**250mm**
Half cone Angle of cone roll	**17.5°**
Rolling time	**120s**
Initial ring temperature	**1150℃**
Tool temperature	**200℃**
Environment temperature	**40℃**
Main roll speed	**19.10r/min**
Friction coefficient	**0.25**

Result and discussion

Deformation law of the forging size. Four moments in the ring blank 3 forging process are depicted in Fig. 5: the beginning of rolling, the moment at which the upper axial roll is pressed down by 30 mm, the moment at which the large hole section of the ring comes into contact with the upper axial roll, and the end of rolling.

At the beginning of rolling, the upper surface of the blank only makes touch with the inner diameter side metal with the upper axial roll at the start of rolling, with a contact length of H0-Hb. In the early stage of rolling, the upper axial roll is pressed downwards, causing an axial height difference between the large and small hole parts of the ring, thereby obtaining the axial depth of the step. A tiny amount of deformation happens as a result of the axial deformation pulling on the metal at the large hole ring. As a result, the ring blank cross-section slopes when the upper axial roll is pressed down by 30 mm, and the step's axial depth is less than the upper axial roll's axial downward pressure. When rolling to D=3002mm, the axial depth of the step is equal to the downward pressure of the top cone roller shaft, and the height of the large hole part of the ring reaches Bb. In the latter stages of rolling, the upper axial roll and mandrel keep feeding, distributing the ring piece's volume in the direction of the large-hole ring, filling the axial roll cavity even more, and shortening the ring piece's upper surface slope. Rolling stops when the ring outer diameter D reaches 3711mm. Based on the simulation findings, it is evident that the key

problem with the forgings' formation is insufficient metal filling at the step, which prevents the Hb value from reaching the design size. Fig. 6 displays the Hb values of two groups of ring blanks.

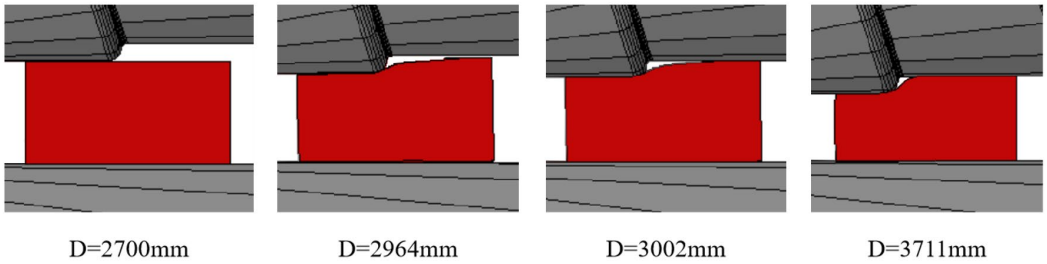

Fig. 5. The forming process of the forging cross-section.

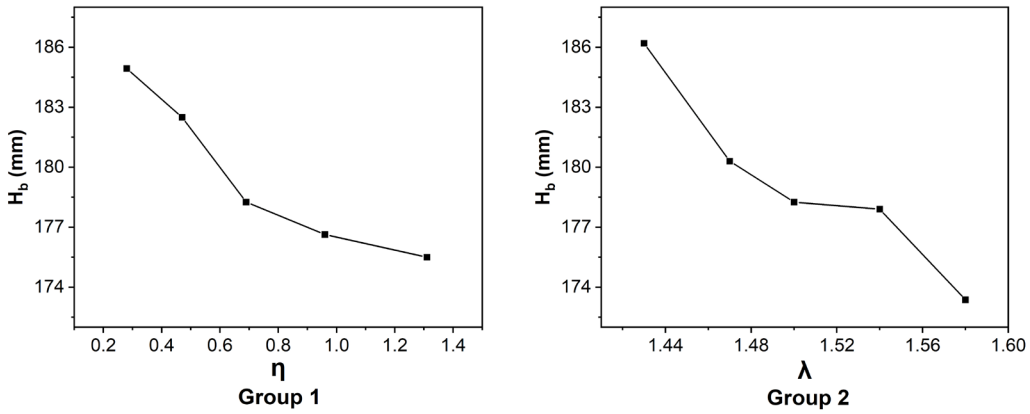

Fig. 6. The H_b values of two groups of ring blanks.

Factors affecting the forming size of the forging

Flow deformation of metals. It is known that when the height of the large hole part of the ring has just reached B_b, the ring needs to continue to grow and fill the step with metal. Fig. 7 shows the variation curve of the axial height of the forging step with the outer diameter of the ring during the rolling process of blank 3. According to the variation law of the axial height of the step, the curve can be divided into two parts: stage I and stage II.

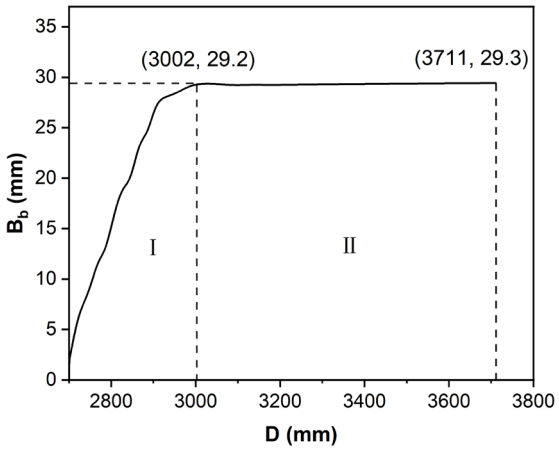

Fig. 7. Variation curve of step's axial height B_b.

As can be seen from the previous text, the proportion of stage II in the total curve has an impact on whether the step filling is sufficient. The proportion relationship is defined as follows:

$$\alpha = \frac{\Delta D_{II}}{\Delta D} = \frac{\Delta D_{II}}{D - D_0}. \quad (5)$$

Where ΔD_{II} is the change in the outer diameter stage II of the ring, and ΔD is the total change in the outer diameter of the ring. Fig. 8 shows the first group of ring blanks' α, It can be observed that the smaller α, the greater the difference between H_b and the design size of 186 mm. Fig. 9 analyzes the metal radial flow deformation behavior of forgings in stage II. It can be seen that the radial plastic strain direction of the forging in the cross-section is opposite, causing the inner and outer diameter metals to flow radially towards the core. At the same time, the direction of axial plastic deformation within the cross-section is consistent, but the amount of metal deformation on the outer diameter side is smaller than that on the inner diameter side, causing the forging metal to flow and fill towards the step. The α of the first group of ring blanks decreases with the increase of η, which is not conducive to the filling at the step, resulting in an increase in the difference between the final H_b and the design size.

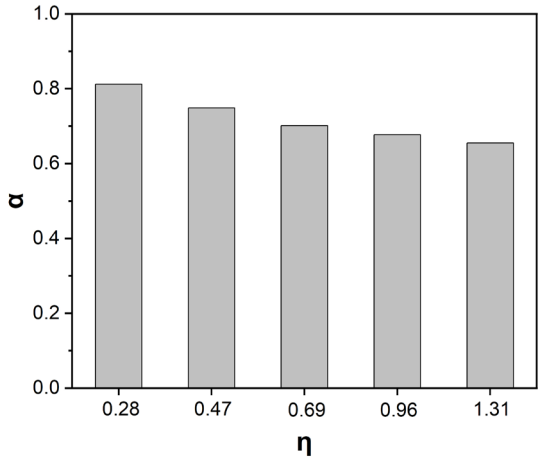

Fig. 8. The influence of radial-to-axial deformation ratio η on the value of α.

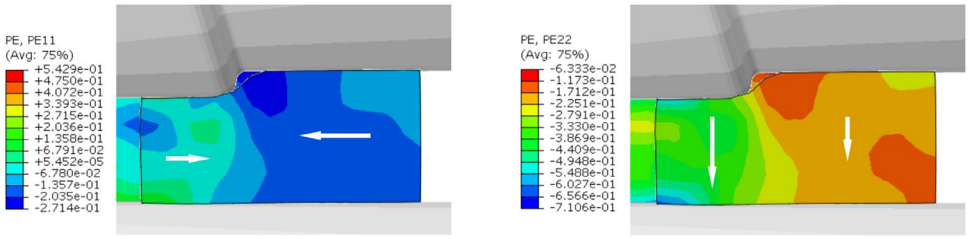

(a) (b)

Fig. 9. Metal flow deformation in stage II: (a)radial plastic strain component; (b) axial plastic strain component.

Control of the roll motion. Compared with the first group of blanks, the second group has a larger variation in rolling ratio, with different ΔD, different deformation speeds, and a greater influence on the forming size by the motion of the rolls.

The motion of the rolls is the key to ensuring the forming size of the forging during rolling. Fig. 9 shows the V_D and V_W during the rolling process of blank 6 and 9. It was found that the matching between V_D and V_W was poor for blank 6 with larger λ. This is because in stage I, only the inner diameter side of blank is in contact with the upper axial roll, and the contact length changes with the wall thickness during the rolling process. In stage II, the axial roll can further adhere to the ring. This change in contact length leads to uneven force distribution on the forging, unstable rolling process, and susceptibility to eccentricity, resulting in a difference between the measured and the actual outer diameter of the ring, which affects the matching between V_D and V_W. Larger λ lead to larger deformation speeds as well, making the matching of V_D to V_W worse and leading to an increase in the difference between Hb and the design dimensions. This problem is also demonstrated by the difference between the setback distance of axial roll ΔL and ΔD for forgings of different λ in Table 5.

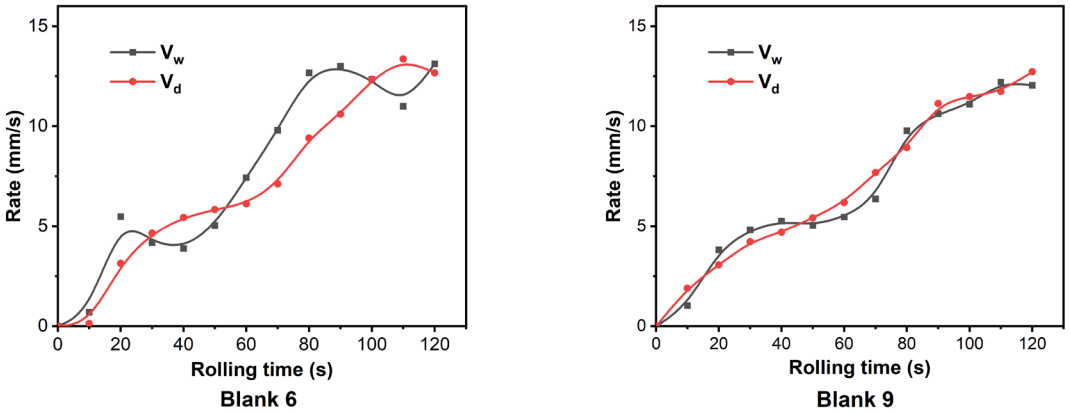

Fig. 9. V_D and V_W during rolling.

Table 5. The difference between ΔL and ΔD (mm).

λ	1.58	1.58	1.50	1.47	1.47
ΔD	1111	1061	1011	961	911
ΔL	1129	1066	1012	960	909
ΔD-ΔL	-19	-5	-1	1	2

Rolling experiment.

In summary, smaller λ and η should be selected for the rolling of L-section ring with profile axial conical rolls. To verify the feasibility of the near-net shape rolling process of L-section ring with profile axial conical rolls, rolling experiment was conducted on a wind power yaw bearing with larger step length. The η used was 0.22, and λ was 1.44, the outer diameter of the ring blank is 2860mm, the inner diameter is 2198mm, the height is 180mm, and the material is 42CrMo. The rolling experiment of the L-section forging is shown in Fig. 10. The rolling process is smooth, and the forming size is good, which verifies the feasibility of the rolling process with profile axial conical rolls.

Fig. 10. Rolling experiment with profile axial conical rolls.

Summary

This article takes an L-section wind power yaw bearing forging as the research object, and conducts research on its near-net rolling forming law and design method. The following conclusions are drawn:

(1) Two groups of blanks with differences η and λ was designed to study the influence of blank size on the near-net rolling forming size of L-section ring with profile axial conical rolls;

(2) When the η increases, the value of α decreases, which is not conducive to filling the step;

(3) The control of roll motion, especially the matching of V_D and V_W, has a significant impact on the forming size of L-section rings. Therefore, a smaller λ is beneficial for improving the matching between V_D and V_W.

Acknowledgment

This research work is supported by the National Key Research and Development Project (2018YFA0702900), Hubei Key Research and Development Project (2022EJD012), Jiangsu Transformation Projects of Scientific and Technological Achievements (BA2022106), China Postdoctoral Foundation Project (2023M742675), 111 Project (B17034) for the supports given to this research.

References

[1] D.S. Qian, L. Hua, Blank design optimization for stepped-section profile ring rolling, J. Sci. China-Technological Sciences 24 (2010) 1612-1619. https://doi.org/10.1007/s11431-010-3113-6

[2] Yu-Min Zhao, D.S. Qian, Effect of rolling ratio on groove-section profile ring rolling, J. Mech. Sci. Tech. 24 (2010) 1679-1687. https://doi.org/10.1007/s12206-010-0525-y

[3] L. Hua, D.Y. Tian, X.H. Han, W. Zhuang, Modelling and analysis of metal flowing behaviors in constraining ring rolling of tapered ring with thin wall and three high ribs, J. Chinese J. Aeronautics 36 (2023) 476-492. https://doi.org/10.1016/j.cja.2023.04.011

[4] L. Liang, L. Guo, Advanced feeding strategy driven by staged growth velocity for groove-section profiled ring rolling, J. Manuf. Process. 81 (2022) 907-921. https://doi.org/10.1016/j.jmapro.2022.07.050

[5] L. Hua, J.D. Deng, D.S. Qian, Recent development of ring rolling theory and technique, Int. J. Mater. Product Tech. 54 (2017) 65-87. https://doi.org/10.1504/IJMPT.2017.080566

[6] I.Y. Oh, T.W. Hwang, Y.Y. Woo, H.J. Yun, Y.H. Moon, Process-induced defects in an L-shape profile ring rolling process, Int. J. Mater. Forming 12 (2019) 727-740. https://doi.org/10.1007/s12289-018-1450-3

[7] P.Z. Zhou, L.W. Zhang, S.D. Gu, J. Ruan, L. Teng, Mathematic modeling and FE simulation of radial-axial ring rolling large L-section ring by shape axial roll, Int. J. Adv. Manuf. Tech. 72 (2014) 729-738. https://doi.org/10.1007/s00170-014-5705-y

[8] D.S. Qian, H Tian, J.D. Deng, Towards Extremely Large-scale Radial-axial Ring Rolling for Constant Ring Growth State with Accurate Closed-loop Control Method, J. Mech. Eng. 59 (2023) 85-95. https://doi.org/10.3901/JME.2023.10.085

[9] X. Li, L. Guo, F. Wang, On a plastic instability criterion for ultra-large radial-axial ring rolling process with four guide rolls, Chinese J. Aeronautics 35 (2022) 391-407. https://doi.org/10.1016/j.cja.2021.07.026

[10] D.S. Qian, B B Ma, J.D. Deng, Numerical simulation and experimental study on grain evolution in whole process of forging and rolling forming—waste heat quenching of 42CrMo ring, Chinese J. Aeronautics 29 (2022) 1-7. https://doi.org/10.3969/j.issn.1007-2012.2022.11.001

[11] L. Hua, X.G. Huang, C.D. Zhu, Theory and Technology of Ring Rolling, first ed., China Machine Press, 2001.